Guy Chavent George Papanicolaou
Paul Sacks William W. Symes
Editors

Inverse Problems in Wave Propagation

With 100 Illustrations

Springer

APPLICATIONS OF INVERSE METHODS TO THE ANALYSIS OF REFRACTION AND WIDE-ANGLE SEISMIC DATA

ROBERT L. NOWACK*

Abstract. The refraction inverse problem was initially investigated by Herglotz (1907), Bateman (1910), and Wiechert and Geiger (1910) who applied Abel transforms for the inversion of seismic travel-times in radially varying media. For smoothly varying media in the absence of low velocity zones, this formulation provides an inverse solution which includes ray bending. In the presence of low velocity zones, bounds on the solution can be obtained from discontinuities in the travel-time data. As an illustration of the inversion of refraction data in radially varying media, slant-stacked wavefield data are used to invert for velocity in the earth's upper mantle. The inversion of wavefield data avoids the picking of travel-times, but requires good quality refraction data which is well sampled in offset. In laterally varying media, an inversion formulation using seismic attributes has been developed. Examples of seismic attributes include envelope amplitudes, instantaneous frequencies, and phase times of selected arrivals. Ray perturbation theory is used to compute the sensitivity of different attributes to variations in the model. To illustrate the inversion of seismic attributes in laterally varying media, attributes extracted from observed refraction data are used to invert for shallow crustal structure. Iterative inversions from smooth to less smooth models are used to progressively incorporate the longer wavelength features of the model.

Key words. Seismic Inversion, Seismic Refraction Analysis

1. Introduction. The inversion of seismic refraction data goes back to the work of Herglotz (1907), Bateman (1910), and Wiechert and Geiger (1910) in which Abel transforms were used to invert for radially varying structure. For smoothly varying media and in the absence of low velocity zones, this approach provides an inverse solution which includes ray bending. When low velocity zones are present, bounds on the solution can be obtained from discontinuities in the travel-time data.

As an illustration of the inversion of refraction data, observed wavefield data is used to invert for velocity in the earth's upper mantle. Slant-stacking and downward continuation of the wavefield data are used to invert for radially varying velocity. The inversion of wavefield data avoids the picking of travel-times, but requires good quality seismic data which is densely sampled in offset.

In laterally varying media, an inversion formulation using seismic attributes has been developed. This incorporates more of the seismic data than just travel-times, but with less sensitivity to noise than complete wavefield inversions. Examples of seismic attributes include envelope amplitudes, instantaneous frequencies, as well as the phase times of selected arrivals. Ray perturbation theory is used to compute the sensitivity of different attributes to variations in the model. When using seismic amplitude

* Department of Earth and Atmospheric Sciences, Purdue University, West Lafayette, IN 47907, This work was partially supported by NSF EAR-9405167.

as an attribute for inversion, attenuation as well as velocity structure of the medium needs to be included. To illustrate the inversion of seismic attributes for laterally varying structure, attributes extracted from observed refraction data are inverted for shallow crustal structure. An iterative inversion from smooth to less smooth models progressively incorporates the longer wavelength features of the model without additional smoothing.

2. Travel-time inversion of refraction data. The inversion of seismic refraction data for radially varying media was initially investigated by Herglotz (1907), Bateman (1910) and Wiechert and Geiger (1910).[1] In these papers, refraction travel-times measured on the earth's surface are utilized to invert for velocity structure using Abel transforms. The resulting formulation is referred to here as the HWB solution.

The travel-time of seismic waves can be written as $T(x) = \int v^{-1} ds$, where v is the wave speed and s is distance along the ray. In radially varying media, the parameter, $p_\Delta = \frac{r \sin\theta}{v(r)}$, is conserved along the ray and is used to index the ray, where θ is the angle from the radial and r is the distance from the earth's center. For vertically varying media, the horizontal slowness, $p = \frac{\sin\theta}{v(z)}$, is conserved along the ray and is used as the ray parameter. The travel-time calculations in radially and vertically varying media are related to each other by an earth flattening transformation (Aki and Richards, 1980).

The ray parameter in vertically varying media can be measured at the surface as the slope of the travel-time curve with range, or $p = dT/dX$. In smoothly varying media, a ray will be horizontal at its bottoming depth, Z_B, for rays returning to the surface. At the ray bottoming depth, $p = v^{-1}(Z_B)$. Thus, by determining p from the slope of the travel-time curve, a portion of the inverse problem is solved providing the velocity at the ray bottoming point. The final step of the refraction inverse problem is to determine the depths of the ray bottoming points.

Instead of using the travel-time integral, Herglotz (1907) used the range integral of the travel-times for inversion. In a vertically varying medium, the range integral can be written

$$X(p) = \int_0^{Z_B} \frac{2p dz}{\sqrt{v^{-2} - p^2}},$$

where the source and receiver are at the surface, and Z_B is the ray bottoming depth. Using Abel transforms, the inverse solution can be written

$$Z(v) = -\frac{1}{\pi} \int_{v_0^{-1}}^{v^{-1}} \frac{X(p) dp}{\sqrt{p^2 - v^{-2}}},$$

[1] English translations of the papers by Herglotz (1907) and Wiechert and Geiger (1910), originally in German, have been made and are available on request.

where v_0 is the velocity at the surface. In a smoothly varying medium and in the absence of low velocity zones, this is a complete solution with ray bending included. The radially and vertically varying formulations of these results are given by Aki and Richards (1980).

After the initial work of Herglotz (1907) and Bateman (1910), Wiechert and Geiger (1910) presented a theoretical development, as well as an application using observed data, for the refraction inverse problem. Wiechert and Geiger (1910) gave primary credit for the solution of the inverse refraction problem using Abel transforms to Herglotz(1907). Wiechert and Geiger were interested in applying the theory to resolve the structure of the earth's interior. However, at this time there were only a few seismic measurements from distant earthquakes. One of the teleseismically recorded earthquakes used by Wiechert and Geiger was the 1906 San Francisco earthquake. The inverse solution they obtained for the earth's upper mantle structure had a linear gradient in velocity down to 1500 km depth, with a less steep gradient below. Wiechert and Geiger interpreted their results by identifying the 1500 km depth as the core-mantle boundary, which is now known to be at a depth near 2885 km. Because of the insufficient data used, their inversion results were not very accurate compared with current earth models. Nonetheless, the theoretical formulation by Wiechert and Geiger, as well as the numerical solution of the inverse problem, was correct.

For straight rays in a spherical earth, the laterally varying tomographic inverse problem can be written in terms of Radon transforms (Chapman, 1987; Nowack, 1991). Early scientific applications of the Radon transform include that of Bracewell (1956) and Cormack (1963) (see also, Deans, 1983; Bracewell, 1995). An English translation of the work by Radon (1917) is given by Deans (1983). In seismology, early tomographic inversions using generalized inversion methods were performed by Aki et al. (1976) (see also, Aki and Richards, 1980). The HWB solution is an inverse algorithm using Abel transforms and specialized to radially varying media. The HWB results predate the work of Radon (1917) and provide an early seismological implementation of seismic inversion (Nowack, 1991). Since the HWB inverse solution uses exact ray trajectories, it is more general than straight ray linearizations for media with radial velocity variations.

When low velocity zones are present in the medium, inversion results using refraction data are non-unique. Because refracted rays cannot bottom in low velocity zones, or LVZ's, a tradeoff occurs between the thickness of an LVZ and the velocity distribution within the LVZ and below. However, from surface measurements of travel-time curve discontinuities, ΔT and ΔX, bounds on the thickness of an LVZ structure can be obtained (Slichter, 1932). A more complete description of non-uniqueness in the presence of LVZ's when using refraction data is given by Gerver and Markuskevitch (1966). A priori constraints on the velocity distribution in an LVZ are usually used to reduce the non-uniqueness. The analysis of surface waves

is commonly assumed to resolve the ambiguity of LVZ structure, but recent numerical experiments by van Heijst et al. (1994) suggest that a practical ambiguity may still exist when using observed surface wave data.

Recently $\tau(p)$, the intercept of the tangent to the travel-time curve as a function of slope p, has been used for seismic inversion. Geometrically, the travel-time can be decomposed as $T(p) = \tau(p) + pX(p)$, where $pX(p)$ is the part of the travel-time associated with the horizontal propagation of the ray and $\tau(p)$ is the part of the travel time associated with the vertical two-way time of the ray (Bessonova et al., 1974). The function $\tau(p)$ is more appropriate than $X(p)$ for inversion since it is more directly related to a depth-like variable. The conversion of $\tau(p)$ to depth for a given bottoming velocity $v = p^{-1}$ completes the inverse problem in smooth and vertically varying media. In the presence of LVZ's, bounds on the resulting velocity depth function are obtained from observed discontinuities $\Delta\tau$ in the $\tau(p)$ curve.

In laterally varying media, one approach for travel-time inversion is to separate the data into common midpoint gathers with $x_{mid} = (x_r + x_s)/2$ and $x_{offset} = (x_r - x_s)/2$, where x_s and x_r are the source and receiver locations. For seismic data densely sampled in midpoint and offset, the velocity can be estimated at each midpoint and depth in a layer stripping or downward continuing fashion. This is conceptually similar to the HWB formulation, but with the laterally varying velocities above accounted for by ray tracing.

With more variable source and receiver spacings, generalized inversion of the travel-time data is usually performed using least squares (Aki et al., 1976; Aki and Richards, 1980). This has been termed the inverse kinematic problem, and more recently seismic tomography. Refraction tomography was applied to Soviet deep seismic sounding data beginning in the 1960's. In these studies both conventional and nuclear explosions were used as sources to study upper mantle structure. An early application of seismic tomography using refraction data was conducted by Alekseev et al. (1971). A survey of Soviet work on seismic tomography is given by Alekseev et al. (1990). A recent tomographic study of mantle structure using earthquake travel-times is given by Dziewonski (1984). A survey of refraction tomography applied to crustal structure is given by Nowack and Braile (1993).

3. Wavefield inversion of refraction data for radial structure. In order to use more of the seismic data and avoid the picking of travel-times, wavefield data can be used to invert for vertically and radially varying velocity structure. One approach to the inversion of wavefield data is to use slant-stacking and downward continuation to image the velocity structure. A slant-stack, or Radon transform, of wavefield data with offset transforms the data to slope p and intercept τ coordinates. The slant-stack of a wavefield gather $y(t, x)$ with a sufficient sampling in offset can written

as

$$s(\tau, p) = \int_{-\infty}^{\infty} y(t = \tau + px, x)dx$$

(see McMechan and Ottolini, 1980).

In vertically varying media, a slant-stacked wavefield can be downward continued to convert the τ variable to depth, and thus solve for velocity with depth. The downward continued wavefield can be written

$$s(z, p) = \int s(\omega, p)e^{-i\omega\psi(z,p)}d\omega,$$

where $s(\omega, p)$ is the Fourier transform of $s(\tau, p)$, and

$$\psi(z, p) = 2\int_0^{z(p)} \sqrt{v^{-2} - p^2}dz$$

(Clayton and McMechan, 1981). Downward continuation can then be used in an iterative procedure in which the velocity function $v(z)$ is updated at each iteration. Convergence is obtained when the velocity function coincides with the locus of large amplitudes of the geometric arrivals on the downward continued wavefield.

To illustrate the use of refraction data to invert for radially varying structure, an inversion of observed wavefield data for upper mantle structure from Erdogan and Nowack (1993) is described. To obtain the long offsets required to study the earth's upper mantle, a common receiver gather was constructed using short period data recorded at the global digital seismic network station, MAJO, in Japan. Shallow earthquakes in the western Pacific were used to construct a common receiver seismic gather for distances up to 4000 km. A map of the area is shown in Figure 1. Earthquakes are noted by small dots. The central circle indicates an angular range of 35 degrees from the station MAJO.

Figure 2A shows the constructed common receiver gather from earthquakes recorded at various distances from the seismic station MAJO. In order to construct this seismic gather, static time corrections were applied to align the first arrivals in order to correct for variable crustal structure. In addition, deconvolution of the first arrival pulses was performed to equalize the pulses shapes from the different earthquakes (Erdogan and Nowack, 1993).

The downward continuation and slant-stack of the wavefield in Figure 2A is shown in Figure 2B. The slant-stack analysis is similar to that performed by Walck and Clayton (1984) except that only a single station was used to construct the wavefield gather rather than a regional seismic array. The final velocity function is shown by the solid line in Figure 2B. This velocity model includes several zones of rapid velocity increases, as well as an upper mantle low velocity zone. An earth flattening transformation

was applied to the velocity model prior to downward continuation (Aki and Richards, 1980). This velocity model predicts the travel-times shown by the solid lines in Figure 2A.

Figure 3A shows a ray theoretical synthetic gather using the velocity model in Figure 2B. The slant-stack and downward continuation of the synthetic wavefield data using the velocity model from Figure 2B is shown in Figure 3B.

The observed and predicted wavefield data in Figures 2A and 3A illustrate several features of seismic refraction data which can occur for both vertically and laterally varying media. These features include rapid increases in the velocity structure resulting in triplications of the geometric arrivals. In vertically varying media, these triplications are unwrapped by the slant-stacking process performed on the wavefield data. However, slant-stacking requires a sufficient sampling in range in order to avoid spatial aliasing. In this example, the variable receiver spacing in the data resulted in some noise in the slant-stacked wavefield. However, there were adequate traces to reconstruct the major locus of energy in the transformed data.

A second feature of refraction wavefield refraction data is the possible occurrence of discontinuities of the geometric arrivals resulting from low velocity zones. A discontinuous pull-back in the predicted travel-times is shown by the solid line in Figure 2A near a range of 1500 km and is associated with the upper mantle low velocity zone. Using ray methods, geometric arrivals from an LVZ are delayed and offset. However, diffractions can also be generated from the top of an LVZ resulting in weak arrivals in front of the geometric arrivals. In laterally varying media, the possibility of leading diffractions has been described by Wielandt (1987). Slant-stacking of good quality wavefield data can be used to isolate the larger amplitude geometric arrivals.

4. Ray perturbation analysis. For the inversion of seismic data in laterally varying media, perturbation or sensitivity analysis giving changes in the data to variations in the model needs to be performed. For initially homogeneous media, ray perturbation results were given by Keller (1962), Moore (1980, 1991) and Norton and Linzer (1982). Farra and Madariaga (1987) utilized ray perturbation theory to compute travel-times and amplitudes in slightly perturbed media from ray calculations in a nearby heterogeneous reference medium. Applications of ray perturbation theory to numerical inversions using travel-times and amplitudes were given by Nowack and Lutter (1988). Interfaces were incorporated by Nowack and Lyslo (1989) and Farra et al. (1989). Nowack and Pšenčík (1991) used the degenerate perturbation theory of Jech and Pšenčík (1989) to derive perturbed ray equations for general, 3-D anisotropic media based on results in a reference 2-D isotropic medium.

Snieder and Sambridge (1992) investigated higher order travel-time

perturbations using a Lagrangian approach. This work showed that for fixed endpoints, the complete second order travel-time perturbation could be obtained from a first order ray perturbation analysis. The second order perturbation analysis was extended by Snieder and Spencer (1993) and Snieder and Sambridge (1993) to general ray coordinates.

The ray equations for the propagation of high frequency seismic energy can be written as

$$\frac{dx_i}{d\tau} = \frac{\partial H}{\partial p_i}, \qquad \frac{dp_i}{d\tau} = -\frac{\partial H}{\partial x_i},$$

where i ranges from 1 to 3 and τ is here the ray sampling parameter along the ray. One choice for H from Farra et al. (1994) is

$$H(\vec{x}, \vec{p}, \tau) = \frac{1}{2} u^{-1}(\vec{x}) h(\vec{x}) [p^2 - u^2(\vec{x})] = 0,$$

where $u(\vec{x})$ refers to slowness, or the inverse wave speed, and $h(\vec{x})$ is a variable stretch of the ray. With this choice of H, the ray equations become

$$\frac{dx_i}{d\tau} = u^{-1} h p_i, \qquad \frac{dp_i}{d\tau} = h \frac{\partial u}{\partial x_i}.$$

The relation between τ and path length s is

$$\frac{ds}{d\tau} = \sqrt{\dot{x}_i \dot{x}_i} = h(\vec{x}).$$

The linearized ray equations can then be written

$$\begin{bmatrix} \delta \dot{x}_i \\ \delta \dot{p}_i \end{bmatrix} = \begin{bmatrix} 0 & u^{-1}(\delta_{ij} - \dot{x}_i \dot{x}_j) \\ \frac{\partial^2 u}{\partial x_i \partial x_j} & 0 \end{bmatrix} \begin{bmatrix} \delta x_j \\ \delta p_j \end{bmatrix} + \begin{bmatrix} 0 \\ R_i^1 + R_i^B \end{bmatrix} + \delta h \begin{bmatrix} \dot{x}_i \\ \partial u / \partial x_i \end{bmatrix}$$

where δu is the slowness perturbation, $R_i^1 = \frac{\partial \delta u}{\partial x_i}$, $R_i^B = \frac{\partial u}{\partial x_i} - \frac{d(u \dot{x}_i)}{ds}$ is the ray bending term and $h = (1 + \delta h)$ is the ray stretch factor term. This form of the equations builds in the linearized eikonal equation, and also $\dot{x}_i \delta \dot{x}_i = 0$. The solution can be written as

$$\begin{bmatrix} \delta x_i(\tau) \\ \delta p_i(\tau) \end{bmatrix} = P(\tau, 0) \begin{bmatrix} \delta x_i(0) \\ \delta p_i(0) \end{bmatrix} + \int_0^\tau P(\tau, \tau') B(\tau') d\tau',$$

where $B(\tau)$ includes the source terms from the linearized ray equations above and $P(\tau, \tau')$ is the linearized ray propagator in the initial medium. The values $\delta x_i(0)$, $\delta p_i(0)$ and δh are determined to satisfy the boundary conditions on the ray (Farra et al., 1994).

The first order phase perturbation can be written as

$$\delta T_1 = \int_0^{s_0} \delta u ds_0 + u_0 \dot{x}_i \delta x_i |_0^{s_0},$$

where the slowness change is integrated along the initial ray, with the addition of a boundary term related to change in the endpoint positions. This result can be obtained using Fermat's principle (Aki and Richards, 1980). The first order phase perturbation allows for a significant computational savings compared to more direct calculations of first order sensitivity of travel-times to model parameters. As a result, most recent tomographic inversion methods use this first order approach, where higher order terms are included in the inversion by iteration.

The second order travel-time term as given by Snieder and Sambridge (1993) can be written

$$\delta T_2 = 1/2 \int_0^{s_0} \delta x_i \left(R_i^{1S} + R_i^B \right) ds_0 + B.T.$$

where $B.T.$ refers to the ray endpoint boundary terms (given in Eqn. (45) of Snieder and Sambridge, 1993). Also,

$$R_i^{1S} = \frac{\partial \delta u}{\partial x_i} - \frac{d}{ds_0}[\delta u \dot{x}_i]$$

is the slowness perturbation term transverse to the ray, and

$$R_i^B = \frac{\partial u_0}{\partial x_i} - \frac{d}{ds_0}[u_0 \dot{x}_i]$$

is the ray bending term used when the initial trajectory is not a true ray.

For the calculation of ray theoretical amplitudes, the dynamic or paraxial ray equations have been developed in ray centered coordinates (Popov and Pšenčík, 1978; Červený and Hron, 1980). The dynamic ray equations have also been applied to more general wavefield calculations, such as Gaussian beam summation and Maslov methods (Červený, et al., 1982; Nowack and Aki, 1984; Červený, 1985; Chapman and Drummond, 1982).

To include ray amplitudes within an inversion, the sensitivity of geometric amplitudes to changes in the model must be developed. Nowack and Lyslo (1989) used ray perturbation methods to obtain perturbed geometric amplitudes by first obtaining perturbed coordinates for the rays. Because of the different factors included in the geometric amplitudes, the perturbed amplitudes were then computed directly along the perturbed rays.

For realistic earth models, observed seismic amplitudes are also affected by the attenuation structure. Anelastic calculations for slightly attenuative media can be obtained by a continuation of elastic wave solutions with the slowness u_e replaced by

$$u_e \rightarrow u(\omega) \left(1 + \frac{i}{2q(\omega)} \right).$$

For an effectively constant q with frequency then

$$u_e \rightarrow u(\omega_r) \left(1 - \frac{1}{\pi q} \ln \left(\frac{\omega}{\omega_r} \right) + \frac{i}{2q} \right),$$

in which ω_r is the reference frequency at which the slowness model refers. This results in a first order, casual q operator (Aki and Richards, 1980). An attenuated pulse is then of the form

$$p(x,\omega) = S(\omega)e^{i\omega(T-\ln(\omega/\omega_r)t^*/\pi)}e^{-\omega t^*/2},$$

where $T = \int u(x,\omega_r)ds$ is the time along the ray, $t^* = \int u(x,\omega_r)q^{-1}(x)ds$ is the attenuation factor along the ray, and $S(\omega)$ is the initial pulse spectrum. In first order attenuation models, T and t^* are often approximately computed along the nearby real rays instead of the true complex rays.

As an alternative, a complex slowness perturbation from a slightly anelastic medium can be written

$$\delta u_c = \delta u + \alpha\left(u_0 + \delta u q_0^{-1} + u_0\delta q^{-1}\right),$$

where $\alpha = -\ln(\omega/\omega_r)/\pi + i/2$. The linearized ray equations above can then be used to compute the ray perturbations from forcing terms $B(\tau,\delta u_c)$ that depend on the complex slowness perturbation. The resulting perturbed rays in the anelastic medium will in general be complex. Complex phase time perturbations are then computed as in the real case but with a complex ray perturbation, as well as a complex slowness perturbation. For amplitudes, complex reflection coefficients and complex geometric spreading also need to be included. As an example, Zhu and Chun (1994) used complex rays to include finite ray effects by introducing a perturbed complex slowness.

In the approach followed here, attenuation is incorporated by computing t^* and the geometric spreading along a nearby real elastic ray. For this case, the first order t^* perturbation to changes in the medium is written

$$\delta t^* = \int \left[\delta u q_0^{-1} + u_0\delta q^{-1}\right] ds_0 + \delta x_i u_0 q_0^{-1}\dot{x}_i|_0^{s_0}$$

$$+ \int \delta x_i u_0 \left[\frac{\partial q_0^{-1}}{\partial x_i} - \dot{x}_i\frac{dq_0^{-1}}{ds}\right] ds_0,$$

where only the $\int u_0\delta q^{-1}ds_0$ term is nonzero if the starting model is elastic with $q_0^{-1} = 0$. When q_0^{-1} is not equal to zero, all terms contribute. For this case the initial and final real trajectories are not valid rays in the anelastic media. In the terminology of Snieder and Sambridge (1993), the last term on the right is actually a second order term. However, this term is first order in the slowness perturbation through the term δx_i, and needs to be included in a first order analysis of t^*.

5. Tomographic inversion of seismic attributes in laterally varying media. In laterally varying media, a formulation using the inversion of seismic attributes has been developed. This approach includes

more of the seismic data than just travel-times, but is less sensitive to noise than complete wavefield inversions. Examples of seismic attributes are envelope amplitudes, instantaneous frequencies, and phase times of selected arrivals.

Procedures for the extraction of seismic attributes include complex trace analysis, as well as more general wavelet analysis. An early application of transient signal analysis was described by Gabor (1964). More recently in geophysics, wavelet analysis has had a resurgence (Goupillard et al., 1984). Using wavelet analysis, transient signals can be analyzed by translation and dilation operations on selected basis wavelets (Daubechies, 1992). This is in contrast with the use of short-time Fourier analysis.

In order to extract seismic attributes from seismic data, the approach followed here is to perform complex trace analysis in which the analytic signal is constructed from a seismic trace. From the analytic signal, the envelope and instantaneous frequency can be determined. Applications of complex trace analysis to seismic data have been described by Taner et al. (1979). It's important to note that the resulting instantaneous frequency is, in general, not equivalent to a spectral frequency. However, when an appropriate weighted average of the instantaneous frequency is performed, the estimate converges to an average of the positive spectral frequencies.

The analytic signal can be written

$$z(t) = y(t) + i\tilde{y}(t),$$

where a Hilbert transform is used to obtain $\tilde{y}(t)$ from $y(t)$. Alternatively, $z(t)$ can be obtained from the positive frequencies of the spectrum of $y(t)$. The signal envelope is then

$$a(t) = \left[y^2(t) + \tilde{y}^2(t)\right]^{1/2},$$

and the instantaneous frequency can be written

$$f_I(t) = \frac{1}{2\pi} \frac{y(t)d\tilde{y}(t)/dt - \tilde{y}(t)dy(t)/dt}{a^2(t) + \epsilon^2},$$

where ϵ^2 is a small damping factor which is used to stabilize the instantaneous frequency when the envelope becomes small. A weighted average of the instantaneous frequency using the squared envelope is also performed to provide added smoothing of the estimate. Figure 4 shows an example of the determination of the complex envelope and instantaneous frequency from an observed seismic trace. For selected seismic phases, the envelope amplitudes, phase times and weighted instantaneous frequencies can be extracted.

In order to obtain values of the attenuation factor t^* a method based on the matching of instantaneous frequencies between observed and attenuated reference pulses was performed by Matheney and Nowack (1995). In this

approach, an attenuated reference pulse is written in the form

$$p(x,t) = p(x_{ref},t) * IFT\left[e^{i\omega(T+\alpha t^*)}\right],$$

where $p(x_{ref},t)$ is a near offset reference pulse, T is the travel time, and $t^* = \int uq^{-1}ds$ is the attenuation factor. The IFT indicates an inverse Fourier transform, the $*$ indicates convolution, and $\alpha = -\ln(\omega/\omega_r)/\pi + i/2$. In order to estimate the attenuation factor, t^*, between the observed trace and the reference pulse, the instantaneous frequencies f_I^{obs} are first determined. The reference pulse is attenuated using a trial estimate of t^{*calc} to obtain f_I^{calc}. An inverse problem is then formulated for t^* as

$$f_I^{obs} - f_I^{calc} \approx \frac{\partial f_I^{calc}}{\partial t^*}(t^* - t^{*calc}).$$

This equation is iteratively solved to find the relative attenuation factors t^* between the observed traces and the near offset reference pulse using the instantaneous frequency values. The procedure approximately removes the effects of the reference pulse spectrum and was found to be more stable than the use of spectral ratios (Matheney and Nowack, 1995).

An example of an observed crustal seismic gather is shown in Figure 5. Although the amplitudes are normalized to unit strength for plotting purposes, estimates of amplitudes as well as instantaneous frequencies can be obtained for the first arrival pulses on the refraction gather. ¿From the values of the instantaneous frequency, estimates of t^* can be obtained using the matching procedure above.

Assuming that seismic attributes, including pulse amplitudes, attenuation factors t^*, and phase times, have been extracted from the seismic wavefield data, then an inversion of these attributes for velocity and attenuation structure can be performed. A linearized relation between changes in the model parameters, δu and δq^{-1}, and data residuals can be written as

$$\begin{bmatrix} \delta T \\ \delta t^* \\ \delta \ln A \end{bmatrix} = \begin{bmatrix} \partial T/\partial u & \partial T/\partial q^{-1} \\ \partial t^*/\partial u & \partial t^*/\partial q^{-1} \\ \partial \ln A/\partial u & \partial \ln A/\partial q^{-1} \end{bmatrix} \begin{bmatrix} \delta u \\ \delta q^{-1} \end{bmatrix},$$

where T is the travel time, t^* is the attenuation factor, and $\ln A$ is the log-amplitude.

All amplitudes are normalized to a reference pulse amplitude for a near offset receiver. The attenuation factor can be incorporated either as a relative or an absolute t^*. The amplitude partials can be written as

$$\frac{\partial \ln A}{\partial u} = \frac{\partial \ln A_g}{\partial u} + \frac{\partial \ln A}{\partial t^*}\frac{\partial t^*}{\partial u}, \qquad \frac{\partial \ln A}{\partial q^{-1}} = \frac{\partial \ln A}{\partial t^*}\frac{\partial t^*}{\partial q^{-1}}$$

where $\ln A_g$ is the geometric spreading component of the log-amplitude related to the velocity, or real slowness model.

A damped inversion is then used to solve the above system of equations, which at the n-th iteration can be written

$$\mathbf{d} - \mathbf{g}(\mathbf{x}_n) = \mathbf{G}_n(\mathbf{x} - \mathbf{x}_n),$$

where $\mathbf{d}$ is the data vector, $\mathbf{g}(\mathbf{x}_n)$ is the solution to the forward problem using the n-th iteration model $\mathbf{x}_n$, and the sensitivity or partial matrix is $\mathbf{G}_n = \partial \mathbf{g}(\mathbf{x}_n)/\partial \mathbf{x}$. The data and model residuals can be normalized as $\mathbf{d}' = \mathbf{C}_d^{-1/2}(\mathbf{d} - \mathbf{g}(\mathbf{x}_n))$ and $\mathbf{x}' = \mathbf{C}_{x_n}^{-1/2}(\mathbf{x} - \mathbf{x}_n)$, where $\mathbf{C}_d^{1/2}$ and $\mathbf{C}_{x_n}^{1/2}$ represent the data and model weight matrices. The inverse problem can then be written as $\mathbf{d}' = \mathbf{G}_n{}'\mathbf{x}'$ with $\mathbf{G}_n{}' = \mathbf{C}_d^{-1/2}\mathbf{G}_n\mathbf{C}_{x_n}^{1/2}$. The solution is obtained by minimizing $(\mathbf{d}' - \mathbf{G}_n{}'\mathbf{x}')^T(\mathbf{d}' - \mathbf{G}_n{}'\mathbf{x}') + \mathbf{x}'^T\mathbf{x}'$, where T represents the conjugate transpose. The solution is of the form

$$\mathbf{x}' = (\mathbf{G}_n{}'^T\mathbf{G}_n{}' + \mathbf{I})^{-1}\mathbf{G}_n{}'^T\mathbf{d}',$$

where the (n+1)-th solution can be written as $\mathbf{x}_{n+1} = \mathbf{x}_n + \mathbf{C}_{x_n}^{1/2}\mathbf{x}'$. This is termed a damped inversion to distinquish it from a more formal stochastic inversion in which the a priori model and model uncertainties remain fixed at each iteration. In the approach here, the model parameterization may change at each iteration. This allows for a small number of model parameters, representing a smooth model, during the initial iterations of the inversion, and then an increasing number of model parameters at higher iterations. The iterative procedure is terminated when the RMS data residuals are within the data errors.

As an illustration, a combined inversion of seismic attributes for laterally varying crustal structure is presented for shallow structure along the northern end of the 1986 Ouachita PASSCAL seismic experiment. An iterative sequence of inversions was performed from smooth to less smooth models. This was done by increasing the number of vertical speed lines in the model at each iteration step. A vertically varying starting model derived from a 1-D inversion was used to start the iterative process. There were 5 nodes with depth down to 3.25 km with 2, 3, 5, and then finally 9 equally-spaced vertical speed lines from 0 to 80 km in range. The resulting model with 9 vertical speed lines had 45 velocity nodes and 45 attenuation nodes. The iterative process was terminated when the RMS data residuals were less than the observed data uncertainties. This type of iterative procedure has the advantage of freezing in the longer wavelength features of the model based on fitting of the data. Although damping was used, more elaborate model smoothing was not used. This iterative procedure was found to be important when performing a simultaneous inversion of different seismic attributes, since attributes, such as amplitudes, were found to be very sensitive to model roughness.

The final inverted velocity model with 9 vertical speed lines is shown in Figure 6A and includes a shallow basin deepening with distance to the

south. This is also imaged in the attenuation, or inverse-q model shown in Figure 6B. The attenuation model has q values as low as 20 near the surface, increasing to values greater than 100 for depths near 3 km. Figure 7A shows the ray diagram for the crustal model shown in Figure 6. Figure 7B shows a comparison between the observed and computed travel-times, and Figures 7C and 7D show the observed and predicted ln-amplitudes and t^* values. Approximately half of the predicted log-amplitudes from this model resulted from the velocity model and half from the attenuation model.

The seismic amplitudes were found to be very sensitive to the model roughness. The sensitivity of ray amplitudes was noted previously by Nowack and Lutter (1988) who suggested that geometric amplitudes could be used to provide smaller scale structure than from the use travel-times alone. This was also concluded by Neele et al. (1993). However, from the observed crustal data ultilized here, the inverted models were required by the observed amplitudes to maintain a relatively smooth character. The ray amplitudes predicted by a large parameter travel-time inversion alone would have fit the travel-time data, but would have predicted ray amplitudes that were too rough compared to the observed amplitudes. This suggested that an iterative procedure from smooth to less smooth models be performed, including amplitudes and t^* values from the beginning of the inversion procedure.

6. Conclusions. The HWB formulation of Herglotz (1907), Bateman (1910) and Wiechert and Geiger (1910) utilizes Abel transforms and constructs the inverse solution in smoothly varying 1-D media using exact ray trajectories. This inverse formulation is more general than straight ray linearizations when applied to radially varying media. In the presence of low velocity zones, bounds on the HWB inverse solution can be obtained from discontinuities of the travel-time curve.

As an illustration of the inversion of refraction data in radially varying media, observed wavefield data has been used to invert for the earth's upper mantle velocity structure. Slant-stacking and downward continuation are used to invert the wavefield data for radially varying velocity structure. The inversion of seismic wavefield data avoids the picking of travel-times and incorporates more of the seismic data, but requires good quality refraction data which is well sampled in offset.

In laterally varying media, an inversion formulation using seismic attributes has been developed. This approach includes more of the seismic data than travel-times, but with less sensitivity to noise than complete wavefield inversions. Seismic attributes include envelope amplitudes, instantaneous frequencies, and phase times of selected arrivals. Instantaneous frequencies are converted to attenuation factors, t^*, using a matching procedure between the data traces and near offset reference pulses. This compensates for the effects of the reference pulse spectrum in the estimation

of the attenuation factors.

To illustrate the inversion of seismic attributes in laterally varying media, observed crustal refraction data have been used to invert for shallow crustal structure. An iterative inversion procedure was performed starting with smooth models and progressing to less smooth models. This type of inversion procedure was found to be important when simultaneously inverting different seismic attributes. Only first order perturbations of the different seismic attributes were used so that the order of perturbation for the different seismic attributes at each iteration would be kept the same. Higher order perturbations of the seismic attributes were then incorporated by the use of multiple iterations.

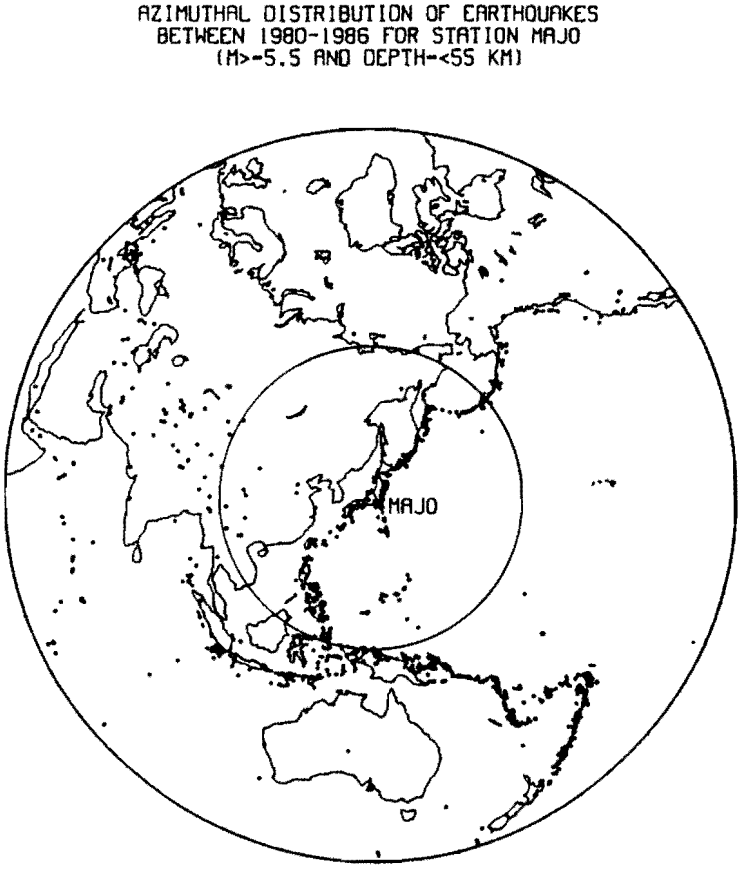

Figure 1. Distribution of earthquake epicenters centered on GDSN station MAJO. The middle circle includes shallow seismicity within 35 degrees of MAJO (from Erdogan and Nowack, 1993).

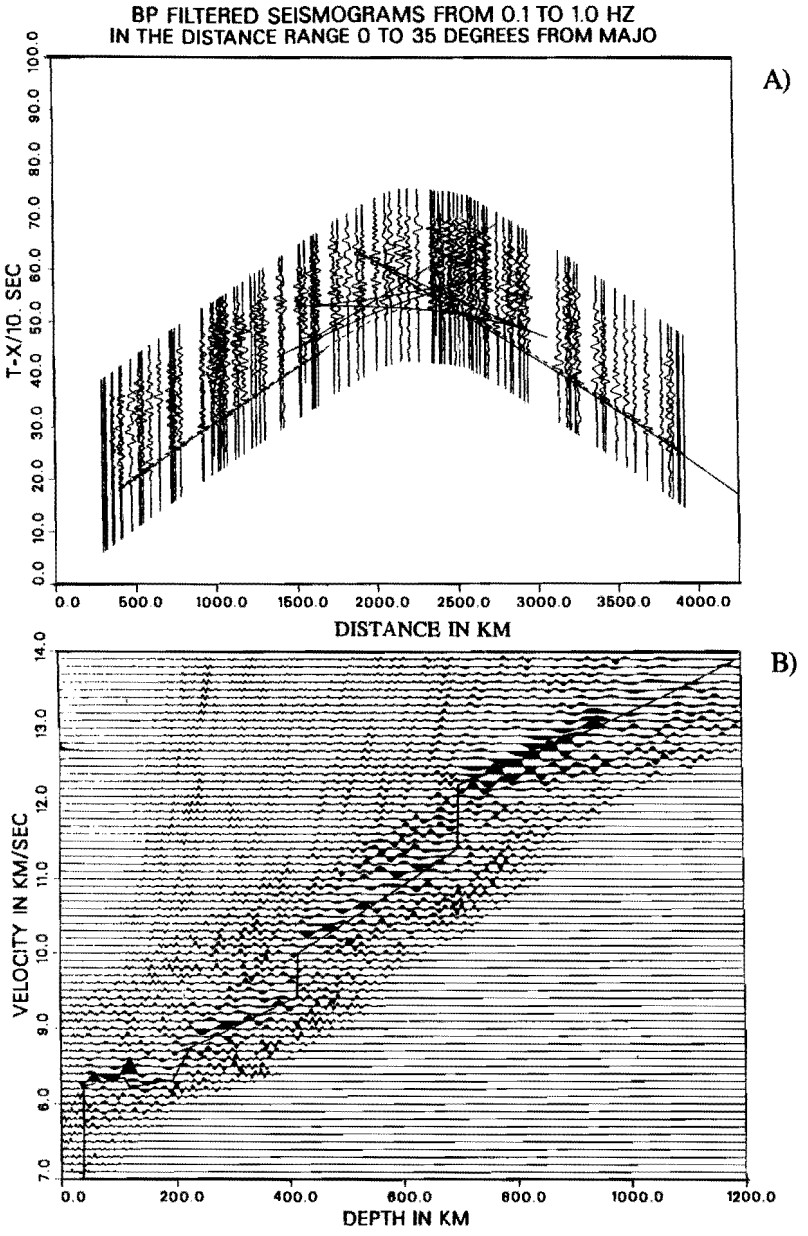

Figure 2. A) Observed seismic wavefield gather with offset from station M in which static corrections and deconvolution have been applied. The solid line is the t predicted from the velocity model shown by the line in B). B) Slant-stacked and downward continued wavefield of the observed wavefield in A). The solid line is the resulting velocity model with an earth flattening transformation applied (modified from Erdogan and Nowack, 1993).

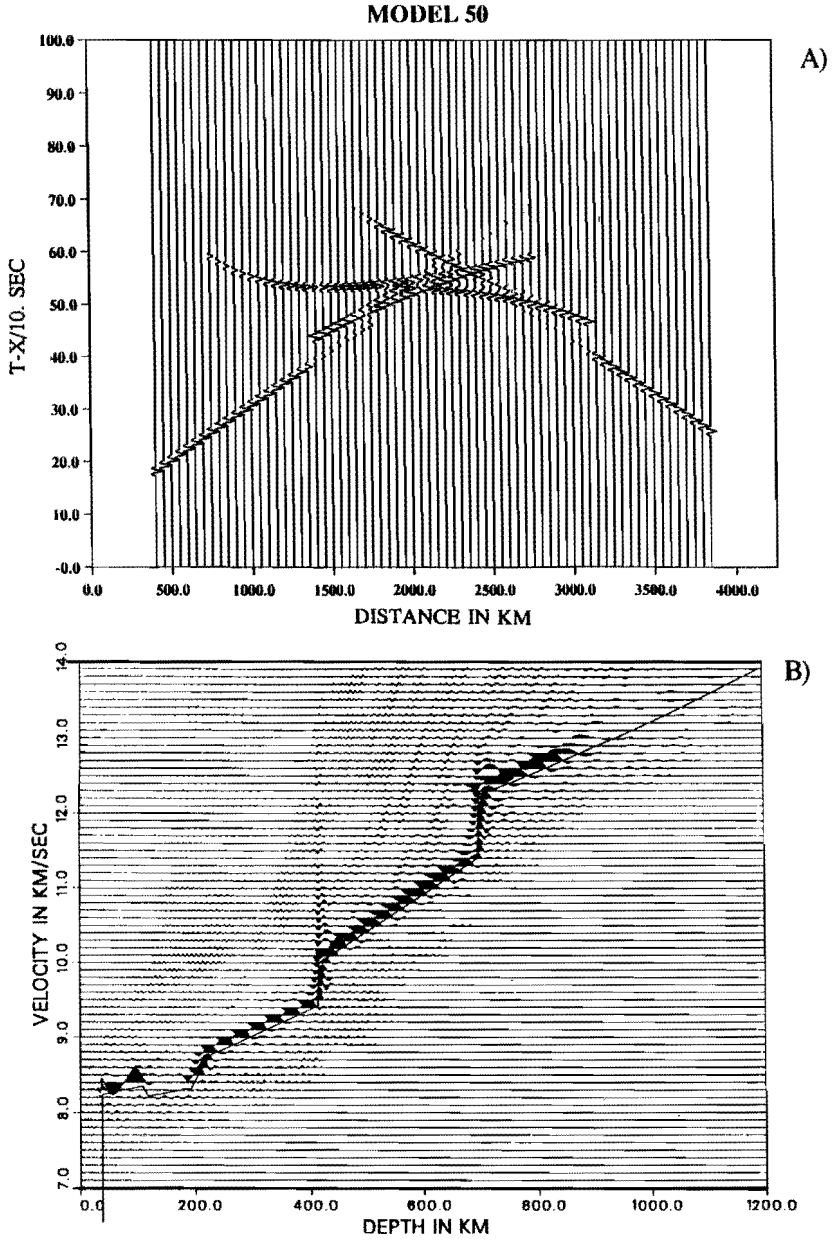

Figure 3. A) Synthetic seismic wavefield computed using the velocity mode in Figure 2B. B) Slant-stacked and downward continuation of the synthetic data A) (modified from Erdogan and Nowack, 1993).

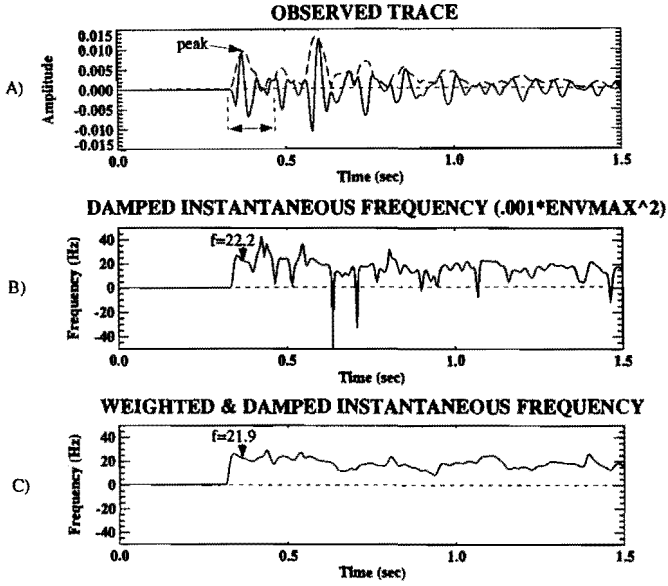

Figure 4. A) An observed seismic trace and its complex envelope. B) Damp instantaneous frequency of the seismic trace in A). C) Weighted and damped instantaneous frequency. For the peak of the first arrival envelope, the instan frequency is noted.

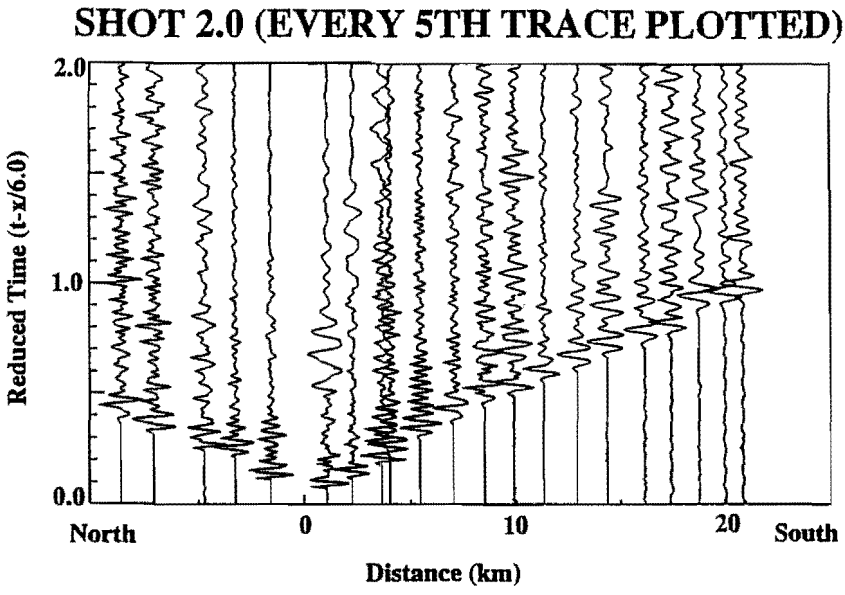

Figure 5. Observed crustal seismic gather displaying wavelet broadening of the first arrivals.

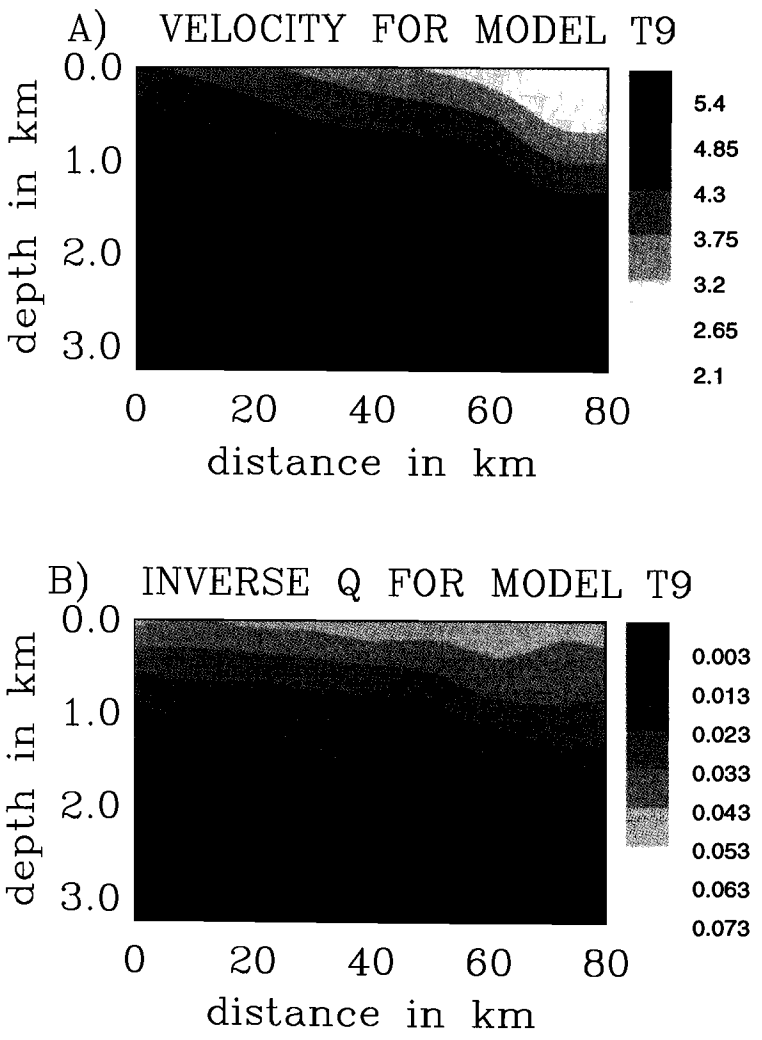

Figure 6. Combined tomographic inversion for velocity and attenuation usi observed crustal seismic attributes. A) Final velocity model using 9 vertical speed lines. B) Final inverse-q model using 9 vertical speed lines.

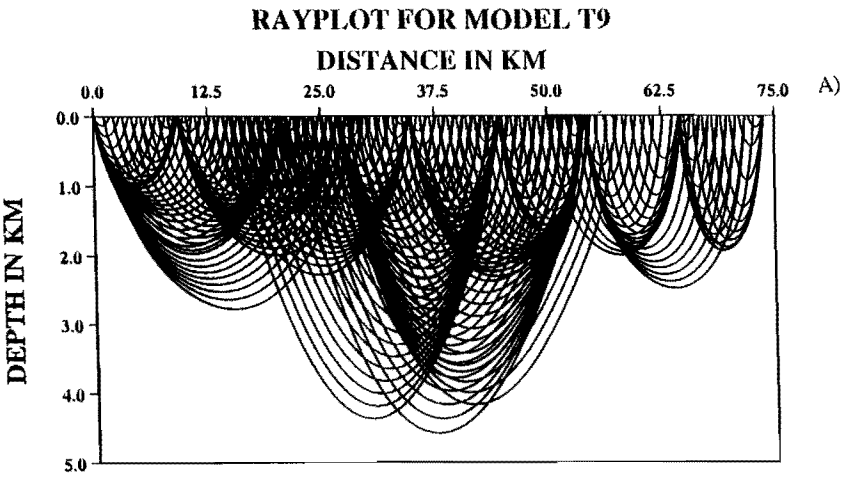

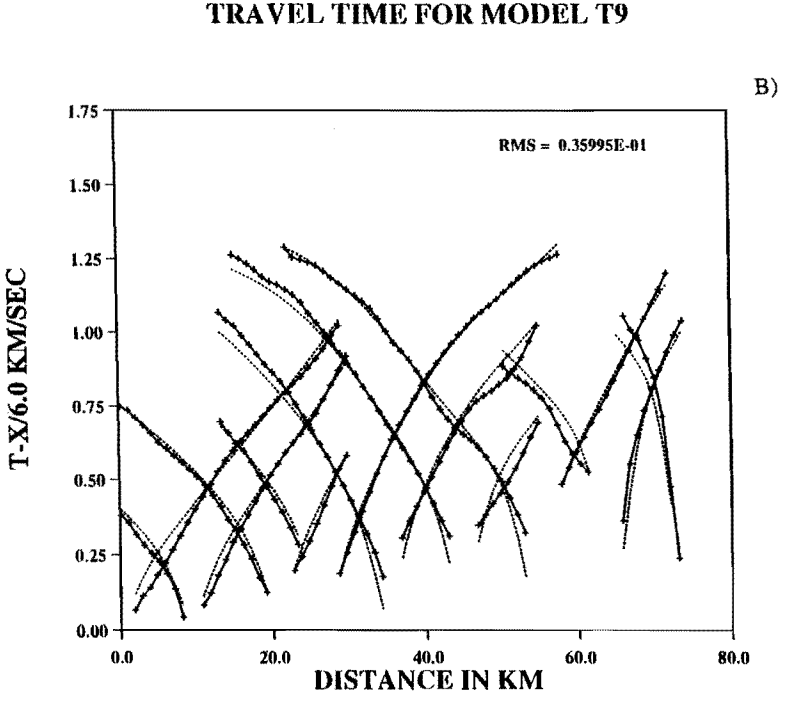

Figure 7. A) The ray diagram for the crustal model shown in Figure 6. B) and computed travel-times for the crustal model shown in Figure 6. The observed data are shown with crosses and the predicted data by dashed lines.

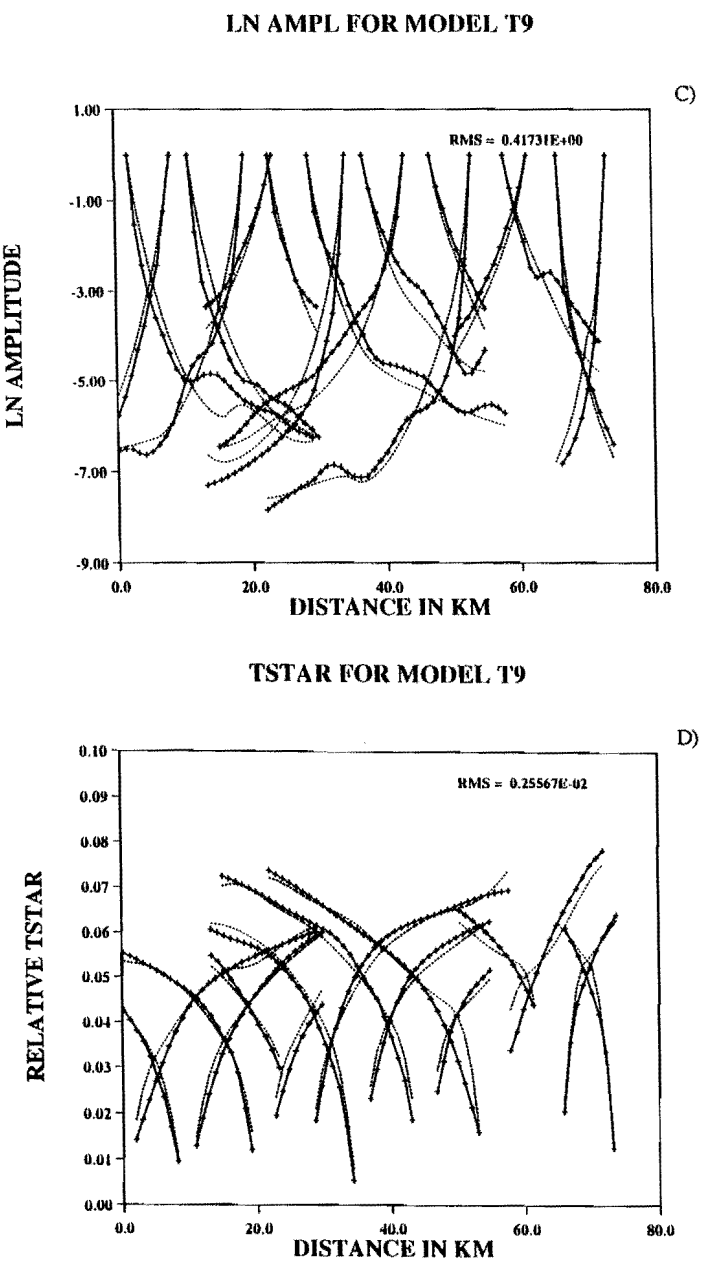

Figure 7 Cont.. C) Observed and predicted ln-amplitudes for the crustal model shown in Figure 6. D) Observed and predicted t^* values.

REFERENCES

[1] K. AKI, A. CHRISTOFFERSSON AND E. S. HUSEBYE, *Determination of the three-dimensional seismic structure of the lithosphere*, J. Geophys. Res., 82 (1976), pp. 277–296.

[2] K. AKI AND P. G. RICHARDS, *Quantitative Seismology Theory and Methods*, W. H. Freeman, San Francisco, 1980.

[3] A. S. ALEKSEEV, M. M. LAVRENTIEV, R. G. MUKHOMETOV, I. L. NERSESOV, AND V. G. ROMANOV, *Numerical method of determination of the structure of the Earth's upper mantle*, in Mathematical Problems of Geophysics, Vol. 2. (eds. M. M. Lavrentiev and A. S. Alekseev), Computing Center, Academy of Science, U.S.S.R. (Siberian Branch), Novosibirsk, (1971), pp. 143–165 (in Russian).

[4] A. S. ALEKSEEV, M. M. LAVRENTIEV, V.G. ROMANOV AND M.E. ROMANOV, *Theoretical and computational aspects of seismic tomography*, Surv. Geophys., 11 (1990), pp. 395–409.

[5] H. BATEMAN, *The solution of the integral equation connecting the velocity of propagation of an earthquake wave in the interior of the Earth with the times which the disturbance takes to travel to the different stations on the earth's surface*, Phil. Mag., 19 (1910), pp. 576–587.

[6] E. N. BESSONOVA, V. M. FISHMAN, V. Z. RYOBOYI, AND G. A. SITNIKOVA, *The tau method for inversion of travel times. I. Deep seismic sounding data*, Geophys. J.R. astr. Soc., 36 (1974), pp. 377–398.

[7] R. N. BRACEWELL, *Strip integration in radio astronomy*, Aust. J. Phys., 9 (1956), pp. 198–201.

[8] R. N. BRACEWELL, *Two-Dimensional Imaging*, Prentice Hall, New Jersey (1995).

[9] V. ČERVENÝ , *Gaussian beam synthetic seismograms*, J. Geophys., 58 (1985), pp. 44–72.

[10] V. ČERVENÝ AND F. HRON , *The ray series method and dynamic ray tracing system for 3-D inhomogeneous media*, Bull. Seism. Soc. Am., 70 (1980), pp. 47–77.

[11] V. ČERVENÝ, M. M. POPOV AND I. PŠENČÍK, *Computations of wavefields in inhomogeneous media - Gaussian beam approach*, Geophys. J.R. astr. Soc., 70 (1982), pp. 109–128.

[12] C. H. CHAPMAN, *The Radon transform and seismic tomography*, in Seismic Tomography, (ed. G. Nolet), Reidel, Dordrecht, (1987), pp. 25–47.

[13] C. H. CHAPMAN AND R. DRUMMOND, *Body-wave seismograms in inhomogeneous media using Maslov asymptotic theory*, Bull. Seism. Soc. Am., 72 (1992), pp. S277–S317.

[14] A. M. CORMACK, *Representation of a function by its line integrals with some radiological applications*, J. Appl. Phys., 34 (1963), pp. 2722–2727.

[15] R. W. CLAYTON AND G. A. MCMECHAN, *Inversion of refraction data by wave field continuation*, Geophysics, 46 (1981), pp. 860–868.

[16] S. R. DEANS, *The Radon Transform and its Applications*, Wiley Interscience, New York, 1983.

[17] I. DAUBECHIES, *Ten Lectures on Wavelets*, SIAM, Philadelphia, 1992.

[18] A. M. DZIEWONSKI, *Mapping the lower mantle: determination of lateral heterogeneity in P velocity up to degree and order 6*, J. Geophys. Res., 89 (1984), pp. 5929–5952.

[19] N. ERDOGAN AND R. L. NOWACK, *Slant-stack velocity analysis for one-dimensional upper mantle structure using short-period data from MAJO*, Pure and Applied Geophys., 141 (1993), pp. 1–24.

[20] V. FARRA AND R. MADARIAGA, *Seismic waveform modeling in heterogeneous media by ray perturbation theory*, Geophys. J.R. Astron. Soc., 76 (1987), pp. 697–712.

[21] V. FARRA, R. MADARIAGA AND J. VIRIEUX, *Comment on "The ambiguity in ray perturbation theory" by Roel Snieder and Malcolm Sambridge*, J. Geophys. Res., 99 (1994), pp. 21963–21968.

[22] V. FARRA, J. VIRIEUX AND R. MADARIAGA, *Ray perturbation theory for interfaces*, Geophys. J. Int., 99 (1989), pp. 2697–2712.

[23] D. GABOR, *Theory of communication*, Proc. Inst. Elect. Eng., 93 (1946), pp. 429–457.

[24] M. L. GERVER AND V. MARKUSHEVITCH, *Determination of a seismic wave velocity from the travel time curve*, Geophys. J.R. astr. Soc., 11 (1966), pp. 165–173.

[25] P. GOUPILLARD, A. GROSSMANN AND J. MORLET, *Cycle-octave and related transforms in seismic analysis*, Geoexploration, 23 (1984), pp. 85–102.

[26] G. HERGLOTZ, *Über das Benndorfsche Problem der Fortpflanzungsgeschwindigkeit der Erdbebenstrahlen*, Phys. Z., 8 (1907), pp. 145–147.

[27] J. JECH AND I. PŠENČÍK , *First order perturbation method for anisotropic media*, Geophys. J. Int., 99 (1989), pp. 369–376.

[28] J. B. KELLER, *Wave propagation in random media*, Proc. Symp. Appl. Math., 13 (1962), pp. 227–246.

[29] M. P. MATHENEY AND R. L. NOWACK, *Seismic attenuation values obtained from instantaneous frequency matching and spectral ratios*, Geophys. J. Int., 123 (1995), pp. 1–15.

[30] G. A. MCMECHAN AND R. OTTOLINI, *Direct observation of a p-tau curve in a slant stacked wavefield*, Bull. Seism. Soc. Am., 70 (1980), pp.775–789.

[31] B. J. MOORE, *Seismic ray theory for lithospheric structures with slight lateral variations*, Geophys. J.R. astr. Soc., 63 (1980), pp. 671–689.

[32] B. J. MOORE, *Seismic rays in media with slight lateral variations in velocity*, Geophys. J. Int., 105 (1991), pp. 213–227.

[33] F. NEELE, J. VANDECAR AND R. SNIEDER, *The use of P wave amplitude data in a joint inversion with travel times for upper mantle velocity structure*, J. Geophys. Res., 98 (1993), pp. 12033–12054.

[34] S. J. NORTON AND M. LINZER, *Correcting for ray refraction in velocity and attenuation tomography: a perturbation approach*, Ultrason. Imag., 4 (1982), pp. 201–233.

[35] R. L. NOWACK, *Tomography and the Herglotz-Wiechert inverse formulation*, Pure and Applied Geophys., 133 (1990), pp. 305–315.

[36] R. L. NOWACK AND K. AKI, *The 2-D Gaussian beam synthetic method: testing and application*, J. Geophys. Res., 89 (1984), pp. 7797–7819.

[37] R. L. NOWACK AND L. W. BRAILE, *Refraction and wide-angle reflection tomography: Theory and results*, in Seismic Tomography: Theory and Practice, (ed. H. M. Iyer and K. Hirahara), Chapman and Hall, London, (1993), pp. 733–763.

[38] R. L. NOWACK AND W. J. LUTTER, *Linearized rays, amplitude and inversion*, Pure and Applied Geophys., 128 (1988), pp. 401–421.

[39] R. L. NOWACK AND J. A. LYSLO, *Frechet derivatives for curved interfaces in the ray approximation*, Geophys. J. Int., 97 (1989), pp. 497–509.

[40] R. L. NOWACK AND I. PŠENČÍK , *Perturbation from isotropic to anisotropic heterogeneous media in the ray approximation*, Geophys. J. Int., 106 (1991), pp. 1–10.

[41] M. M. POPOV AND I. PŠENČÍK , *Computation of ray amplitudes in inhomogeneous media with curved interfaces*, Studia Geophys. Geol., 22 (1978), pp. 248–258.

[42] J. RADON, *Über die Bestimmung von Funktionen durch ihre Integralwerte längs gewisser Mannegfaltigkeiten*, Akadamic der Wissenschaften, Leipzig, Math.-Phys. Kl., 69 (1917), pp. 262–267.

[43] L. B. SLICHTER, *The theory of the interpretation of seismic travel time curves in horizontal structures*, Physics, 3 (1932), pp. 273–295.

[44] R. SNIEDER AND M. SAMBRIDGE, *Ray perturbation theory for traveltimes and ray paths in 3-D heterogeneous media*, Geophys. J. Int., 109 (1992), pp. 294–322.

[45] R. SNIEDER AND M. SAMBRIDGE, *The Ambiguity of ray perturbation theory*, J. Geophys. Res., 98 (1993), pp. 22021–22034.

[46] R. SNIEDER AND C. SPENCER, *A unified approach to ray bending, ray perturbation and paraxial ray theories*, Geophys. J. Int., 115 (1993), pp. 456–470.

[47] M. T. TANER, F. KOEHLER AND R. E. SHERIFF, *Complex seismic trace analysis*, Geophysics, 44 (1979), pp. 1041–1063.

[48] H.J. VAN HEIJST, R. SNIEDER AND R.L. NOWACK, *Resolving a low velocity zone with surface-wave data*, Geophys. J. Int., 118 (1994), pp. 333–343.

[49] M. WALCK AND R. CLAYTON, *Analysis of upper mantle structure using wave field continuation of P waves*, Bull. Seism. Soc. Am., 74 (1984), pp. 1703–1719.

[50] E. WIECHERT AND L. GEIGER, *Bestimmung des weges der Erdbebenwellen im Erdinnern*, Phys. Z., 11 (1910), pp. 294–311.

[51] E. WIELANDT, *On the validity of the ray approximation for interpreting delay times* in Seismic Tomography, (ed. G. Nolet), Reidel, Dordrecht, (1987), pp. 85–98.

[52] T. ZHU AND K.-Y. CHUN, *Complex rays in elastic and anelastic media*, Geophys. J. Int., 118 (1994), pp. 181–193.